PRECIPITATION HARDENING IN AS-CAST AA6082 AND AA5754 COMMERCIAL ALLOYS WITH Sc, Zr-ADDITION

Michal LEIBNER [1], Martin VLACH [1], Veronika KODETOVÁ [1], Bohumil SMOLA [1], Marián VLČEK [1], Tomáš KEKULE [1], Ivan PROCHÁZKA [1], Hana KUDRNOVÁ [1], Vladivoj OČENÁŠEK [2]

[1]*Charles University, Faculty of Mathematics and Physics, Ke Karlovu 3, Prague, Czech Republic, EU*
mleibner@seznam.cz

[2]*SVÚM a.s., Tovární 2053, Čelákovice, Czech Republic, EU*

Abstract

The as-cast AA5754 and AA6082 alloys with Sc,Zr-addition were investigated during isochronal annealing from room temperature up to 510 °C. Precipitation reactions were studied by electrical resistivity, hardness measurements and differential scanning calorimetry. The measurements were compared to microstructure development that was observed by transmission electron microscopy. Higher initial resistivity as well as hardness values are probably caused by a higher content of the solutes in the AA5754-ScZr alloy in comparison with the latter alloy. Both alloys contains spherical particles of the $Al_3(Sc,Zr)$ phase in the as-cast state. Moreover, the AA6082-ScZr alloy contains Mg,Si,Sc-containing phase at grain boundaries and rods/needles of the Mn,(Fe)-containing phase. The transient Al-Mg-Si-phase (*β*'' and/or *β*') particles formed during isochronal annealing in the AA6082-ScZr alloy cause a poor age hardening. The additional $Al_3(Sc,Zr)$ particles precipitation causes a pronounced hardening in the AA5754-ScZr alloy. The possible (weak) additional precipitation of the $Al_3(Sc,Zr)$ particles in the AA6082-ScZr alloy has a lower effect on hardness than the precipitation of *β*'' and *β*' phases or Sc and Zr solutes are probably bound in the $Al_3(Sc,Zr)$ particles and do not influence precipitation hardening in the course of isochronal annealing in the AA6082 alloy. The precipitation of the $Al_6(Mn,Fe)$-phase was observed in the alloys during the isochronal heat treatment. The apparent activation energy values of precipitation of the transient *β*'' and/or *β*' phases, $Al_6(Mn,Fe)$-phase and $Al_3(Sc,Zr)$ phase were determined.

Keywords: Electrical resistivity, DSC, TEM, Al-Mg-Si system, $Al_3(Sc,Zr)$ phase

1. INTRODUCTION

Al-based alloys are very preferred for automotive manufacture to produce lightweight vehicles [1-3]. After designing Al-Sc-Zr-based alloys, typically ~0.2 wt.% Sc, ~0.1 wt.% Zr, an effort was put into investigation of the effect of Sc and Zr addition to commercial Al hardenable alloys [1, 4]. A simultaneous addition of Sc and Zr is probably the most effective element combination having an antirecrystallization impact in Al due to precipitation of the $Al_3(Sc,Zr)$ phase with $L1_2$ structure [1, 4]. The Al-Mg-based alloys exhibit a reasonable solid solution hardening, but only a poor age hardening [3, 4]. Al-Mg-Si-based alloys are widely used as structural materials in automotive and aviation industry [5]. Mixture of Mn, Cr and Fe is the most widely used combination of metals in commercial Al-based alloys [1, 5, 6]. Properties of the Al-based alloys (AA5XXX and 6XXX series) logically depend on chemical composition, mainly on Mg and Si content and on the heat treatment of the studied alloys [4-6]. Despite a number of investigations of Al-Mg-, Al-Mn-, Al-Mg-Si- as well as Al-Sc-Zr-based alloys there are considerably less systematized data about the effect of Sc,Zr-addition on phase transformation in the commercial Al-based alloys. An understanding of the complex interactions between concurrent precipitation processes requires further investigation [5, 6, 8]. A tailoring of the material with required properties is very difficult without the detailed knowledge of precipitation processes and the role of Sc and Zr in microstructure development.

2. MATERIALS AND METHODS

The as-cast Al-3.5 wt.% Mg-0.3 wt.% Mn-0.2 wt.% Si-0.2 wt.% Fe-0.1 wt.% Cu-0.1 wt.% Cr-0.25 wt.% Sc-0.12 wt.% Zr (AA5754-ScZr) and Al-0.8 wt.% Mg-0.7 wt.% Mn-0.9 wt.% Si-0.2 wt.% Fe-0.1 wt.% Cu-0.1 wt.% Cr-0.20 wt.% Sc-0.11 wt.% Zr (AA6082-ScZr) alloys were studied. The temperature ranges of phase transformations in the alloys were determined by electrical resistivity (measured at 77 K) and hardness (HV10) measurements (measured at 295 K) from room temperature (RT) up to 510 °C. The annealing was carried out in an oil bath (up to 240 °C) or in a furnace with protective atmosphere (at higher temperatures); each annealing step was finished by a quenching. Samples of the alloys for resistivity and hardness measurements were studied during the isochronal annealing procedure (steps of 30 K / 30 min) which was performed exactly in the same way as described in [6, 8].

The thermal behaviour of the alloys were studied using by differential scanning calorimetry (DSC) performed at heating rates of 1, 2, 5, 10, 20 and 30 K·min^{-1} in the Netzsch DSC 204 F1 Phoenix apparatus. A specimen of mass between 10-20 mg was placed in Al_2O_3 crucibles. Nitrogen flowed at the rate of 40 ml/min as a protective atmosphere.

The measurements mentioned above were compared to microstructure development observed by transmission electron microscopy (TEM) microscopy. TEM observations were carried out in JEOL JEM 2000FX microscope to determine the microstructure of the alloys. The analysis of precipitated phases was complemented by energy-dispersive spectroscopy (EDS) performed by X-ray BRUKER microanalyser.

3. RESULTS AND DISCUSSION

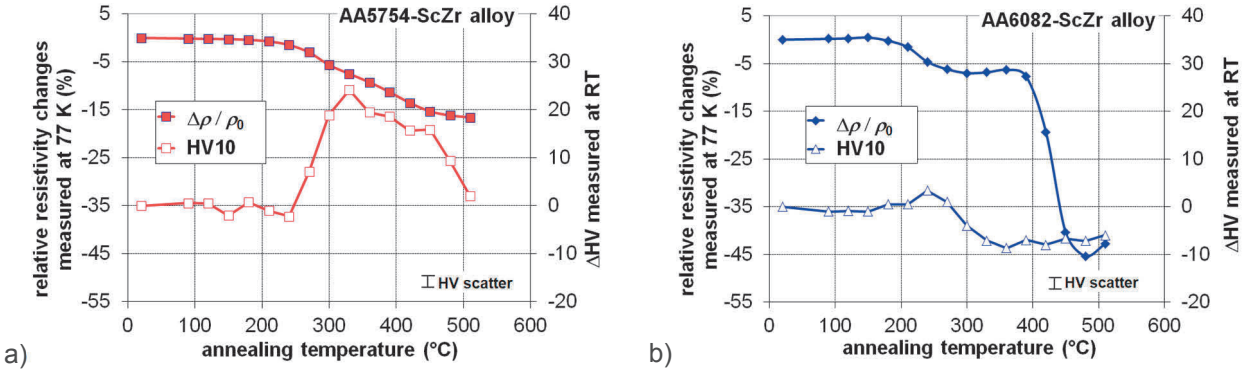

Figure 1 Isochronal annealing curves of relative resistivity changes (measured at 77 K) and hardness ΔHV10 changes (measured at RT): a) AA5754-ScZr alloy, b) AA6082-ScZr alloy.

The response of the relative resistivity $\Delta\rho / \rho_0$ and hardness ΔHV10 changes to step-by-step isochronal annealing in the AA5754-ScZr and AA6082-ScZr alloys are shown in **Figure 1**. The initial values of absolute resistivity values were calculated as ~ 41 nΩ·m for the AA5754-ScZr alloy and ~ 29 nΩ·m for the AA6082-ScZr alloy, respectively. Higher initial resistivity value is probably caused by a higher content of the solutes in the AA5754-ScZr alloy. The different initial values of hardness HV10 of the AA5754-ScZr alloy (HV10 = 85±4) compared to the AA6082-ScZr alloy (HV10 = 71±4) probably reflect also an effect of solutes content.

The resistivity annealing curve of the AA5754-ScZr continuously decreases up to the end of the annealing. No changes in hardness during the annealing up to ~240 °C were observed. HV10 increases in the temperature range of 240-330 °C, after that the HV10 values of the alloy decrease significantly.

The electrical resistivity curve for the AA6082-ScZr alloy exhibits two distinct resistivity stages. Resistivity decreases in the first stage in the temperature range 200-300 °C and it corresponds to a slight peak in

hardness. The main decrease of electrical resistivity is realized in the temperature range 390-480 °C but this process does not lead to a distinct precipitation hardening (see **Figure 1**).

Both as-cast alloys contain the $Al_3(Sc,Zr)$ particles with the $L1_2$ structure [6, 8]. No other particles were observed in the AA5754-ScZr alloy [8]. However, the sample of the AA6082-ScZr alloy also contains rods and needles of the Mn(,Fe,Si)-containing phase with the size of ~ 500 nm. No weak diffraction spots enabling identification of crystallographic structure of this phase were detected in electron diffraction (ED) patterns. This is consistent to the results from Ref. [6]. An overview of the AA6082-ScZr alloy is shown in **Figure 2** (notice weak reflections of the $L1_2$ phase in ED pattern).

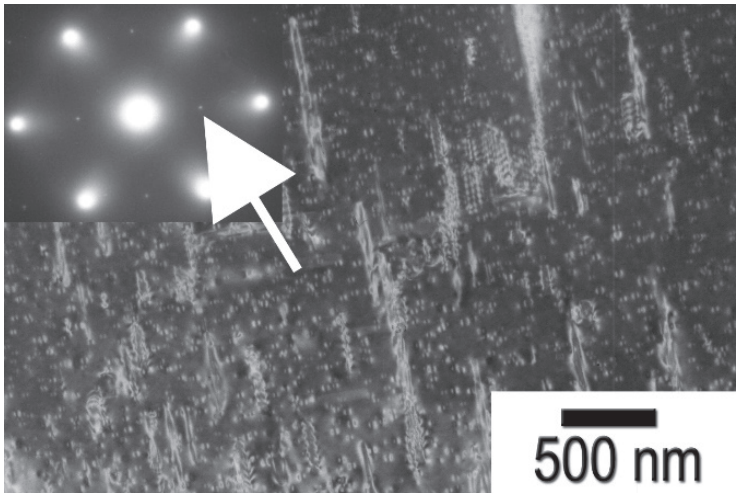

Figure 2 TEM image of the AA6082-ScZr alloy in the as-cast state. See small particles of the $Al_3(Sc,Zr)$ phase and rods and needles of the Mn(,Fe,Si)-containing phase.

The DSC measurements were done in the alloys in addition to electrical resistivity and hardness HV10 measurements. Two exothermal processes (labelled as I-effect and II-effect) in both alloys were detected. The maximum heat flow for heating rate 1 K/min was observed at characteristic temperatures T_f equal to ~292 °C, ~400 °C in the AA5754-ScZr alloy and ~237 °C, ~413 °C in the AA6082-ScZr alloy, respectively. With increasing heating rates the temperature T_f is shifted to higher temperatures. The DSC exothermic peaks of the I-effect correspond to the hardness increase in the AA5754-ScZr (~300 °C) and AA6082-ScZr alloy (~ 240 °C), respectively. On the basis of the obtained results, the apparent activation energy for individual processes was determined by the Kissinger method [9] (see **Figure 3**) in the coordinate system of $[\ln(\delta / T_f^2); 1 / T_f]$, where δ is the heating rate with the result of Q_I = 120±6 kJ·mol^{-1}, Q_{II} = 180±20 kJ·mol^{-1} for the AA5754-ScZr alloy and Q_I = 120±20 kJ·mol^{-1}, Q_{II} = 170±20 kJ·mol^{-1} for the AA6082-ScZr alloy, respectively.

Precipitation of the needle-shaped β'' phase and/or rod-shaped β' phase from the Al-Mg-Si system in the AA6082-ScZr alloy was observed by TEM after isochronal annealing up to ~240 °C (see **Figure 4**). This is the reason of the peak hardening at this temperature range. The peak hardening is very poor (~5 %) which was also observed in a cast AlMgSiMn alloy of a similar composition (~12 %) [6]. However, there is also another explanation, namely that Mg, Si and Sc are mainly incorporated in the Al(Mg,Si,Sc)-containing phase (see **Figure 4**) which is formed after casting. Therefore Mg, Si and Sc are probably excluded from the possible precipitation formation. These particles can also be large enough to get out of the TEM film during polishing.

The calculated apparent activation energy for the I-effect in the AA6082-ScZr alloy is comparable to the values for the transient Mg-Si phase formation that were reported for the alloys without Sc,Zr-addition in literature (65-128 kJ/mol) [6, 10]. It is good noticing that particles of the $Al_3(Sc,Zr)$ phase persist unchanged during the annealing in both alloys. No microstructural changes were observed in the AA5754-ScZr alloy annealed up to 240 °C.

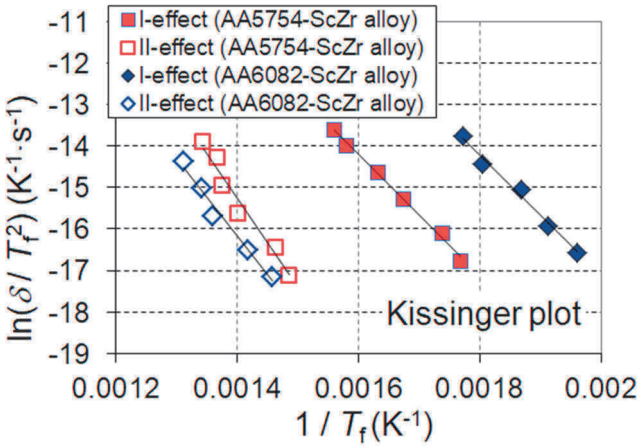

Figure 3 Kissinger plot in the coordinate system of [ln(δ / T_f^2); 1 / T_f] of the effects in the AA5457-ScZr and AA6082-ScZr alloy

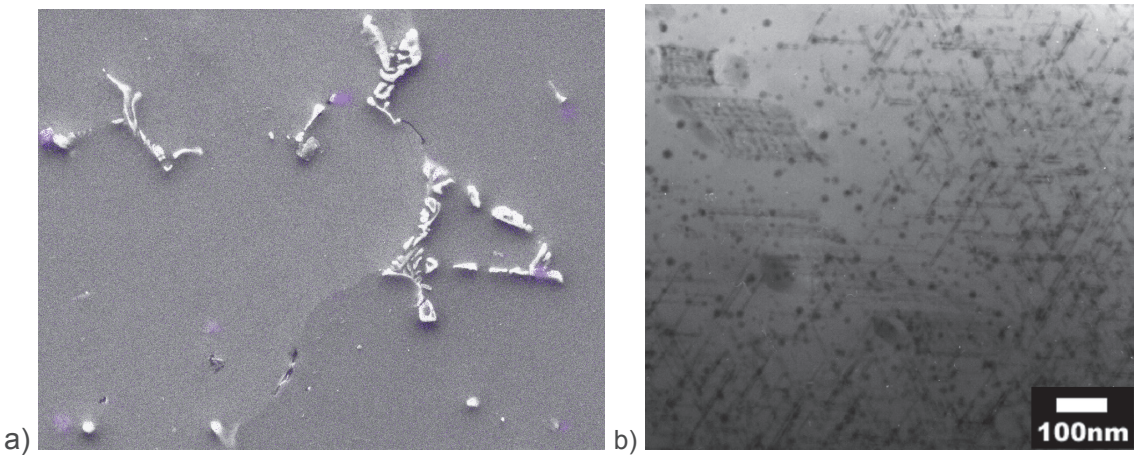

Figure 4 a) SEM image of the AA6082-ScZr alloy in the as-cast state. See the areas with a high total Mg,Si,Sc content. b) TEM image of the AA6082-ScZr alloy isochronally annealed up to 240 °C. See particles of the Al_3(Sc,Zr) phase and needle-shaped β'' phase and/or rod-shaped β' phase from the Al-Mg-Si system.

Temperature position of the hardness increase in the AA5754-ScZr (~ 300 °C) does not differ from that observed in the Al-Sc-Zr as well as Al-Mn-Sc-Zr alloys [1]. This hardening was found to be caused by an additional precipitation of the Al_3(Sc,Zr) particles. Moreover, in our previous study (see Ref. [8]) an additional precipitation of the $L1_2$-structured Al_3(Sc,Zr) particles in a very weak contrast was detected by TEM and ED in the cold-rolled AA5754-ScZr alloy isochronally annealed up to 330 °C. This dispersion causes the observed a slight increase of the conductivity and pronounced hardening in the cold-rolled alloy at this temperature range (240-330 °C) [8]. No other precipitates were observed in the cold-rolled AA5754-ScZr alloy at 300 °C [8]. Thus it is highly probable that the slight resistivity decrease and hardness increase can be ascribed to this process in the as-cast AA5754-ScZr alloy, too. This conclusion also supports the fact that the calculated value of the activation energy *Q* of the observed I-effect in the AA5754-ScZr alloy is comparable within experimental scatter to the apparent activation energy *Q* for precipitation of the Al_3(Sc,Zr) phase in the Al-Mn-Sc-Zr alloy 116±9 kJ·mol^{-1} as well as in the cold-rolled AA5754-ScZr alloy 113±8 kJ·mol^{-1}[6, 8]. From these facts one can also conclude that the possible (weak) additional precipitation of the Al_3(Sc,Zr) particles in the AA6082-ScZr alloy has a lower effect on hardness than the precipitation of β'' and β' phases and/or Sc and Zr solutes are probably (mainly) bound in the Al_3(Sc,Zr) particles and do not influence precipitation hardening in the course of isochronal annealing in the AA6082 alloy.

The main resistivity decrease in the AA6082-ScZr alloy starts at ~390 °C (see **Figure 1b**). With respect to the solubility limits of Mg, Si, Fe, Sc and Zr at comparable temperatures [1], it is obvious that the resistivity development in the AA6082-ScZr alloy at annealing temperatures above ~360 °C must be mainly associated with the other solutes. Indeed, a dense precipitation of oval orthorhombic Al_6Mn phase (or its modifications ($Al_{12}Mn_3Fe_3$, $Al_6(Mn,Fe)$ and $Al_6(Mn,Fe,Si)$) with the size of 10-100 nm was observed by TEM (see **Figure 6a** in Ref. [6]). In our previous study (Ref. [6]) it was also observed that the precipitation of the Mn-containing particles has a negligible effect on hardness contrary to particles of the β'' and β' phases from the Al-Mg-Si system. The assumption of the Al_6Mn particle formation is confirmed by the calculated apparent activation energy value Q_{II} = 170±20 kJ·mol^{-1} in the studied AA6082-ScZr alloy - the value corresponds very well to the value for Al_6Mn-phase precipitation 162±22 kJ·mol^{-1} in the cold-rolled AlMnScZr alloy [6] and also to the value 166±16 kJ·mol^{-1} reported for cold-rolled AA5754-ScZr alloy [8].

Now, we should note that the resistivity as well as hardness curves of the AA5754-ScZr alloy at temperatures above ~ 330 °C exhibit a continuous decrease (see **Figure 1a**). It must be mentioned that in the 5754-typed Al commercial alloys the precipitation sequence of the Al-Mg and/or Al-Mg-Si system can be observed [4, 6]. On the other hand the precipitation of the Mn,Fe,Cr-containing particles was observed in the AA6082-typed commercial alloys [6]. In view of the fact that the precipitation of the Mn(,Fe,Cr)-containing as well as Mg-containing (e.g. Al_3Mg_2 phase) particles has no significant effect on hardness [6] the changes in resistivity and hardness curves of the studied AA5754-ScZr alloy at temperatures above ~360 °C are probably connected with precipitation of the particles containing Mg (from Al-Mg system) and Mn,Fe,Cr-containing particles with a concurrent coarsening of the $Al_3(Sc,Zr)$ particles. The value (as well as temperature range) of the apparent activation energy of the II-effect (see **Figure 3**) in the AA5754-ScZr alloy agrees with the activation energy for precipitation of the Mn-contaning particles. It indicates that the Mn(,Fe,Cr,Si)-containing particle precipitation prevails over the others, e.g. the apparent activation energies for the precipitation of metastable and/or stable Al_3Mg_2 and/or Mg_2Si phase were observed lower during linear heating 70-140 kJ·mol^{-1}. Unfortunately, the activation energy must be identified with individual nucleation and growth steps in a transformation. Owing to the possible overlapped effects, the exact positions of the beginning and ending of the for example thermal peaks cannot be determined. Thus, the analysis of the activation energy of the II-effect in the studied AA5754-ScZr alloy above ~ 360 °C becomes uncertain. Due to the large number of admixtures, the character of precipitation changes in the studied alloys cannot be described in detail only on the basis of resistivity, thermal and hardness measurements. More (especially microstructural) research is needed to determine specific phase transformations.

4. CONCLUSIONS

Results of characterization of the commercial AA5754 and AA6082 alloys with Sc,Zr-addition by electrical resistometry, thermal analysis, hardness testing and electron microscopy, can be summarized in the following points:

- Higher initial resistivity as well as hardness values are probably caused by a higher content of the solutes in the AA5754-ScZr alloy in comparison with AA6082-ScZr alloy.
- The as-cast alloys contains spherical particles of the $Al_3(Sc,Zr)$ phase. Moreover, the as-cast state of the AA6082-ScZr alloy contains rods and needles of the Mn,(Fe)-containing phase.
- The transient Al-Mg-Si-phase (β'' and/or β') particles formed during isochronal annealing in the AA6082-ScZr alloy cause a poor age hardening. The additional $Al_3(Sc,Zr)$ particles precipitation causes pronounced age hardening in the AA5754-ScZr alloy. The possible (weak) additional precipitation of the $Al_3(Sc,Zr)$ particles in the AA6082-ScZr alloy has a lower effect on hardness than the precipitation of β'' and β' phases. It is also possible that Sc and Zr solutes are probably bound in the $Al_3(Sc,Zr)$ particles and do not influence precipitation hardening in the course of isochronal annealing in the AA6082 alloy.

- The apparent activation energy value of precipitation of the transient *β*'' and/or *β*' phase was determined as 120±20 kJ·mol^{-1} in the AA6082-ScZr alloy.
- The apparent activation energy value of precipitation of $Al_3(Sc,Zr)$ phase was determined as (120 ± 6) kJ·mol^{-1} in the AA5754-ScZr alloy.
- The pronounced precipitation of the $Al_6(Mn,Fe)$-phase was observed in the alloys during the isochronal heat treatment. The apparent activation energy for the $Al_6(Mn,Fe)$-phase precipitation was determined as ~175 kJ·mol^{-1}. Nevertheless, the precipitation of these particles has a negligible effect on hardness.

ACKNOWLEDGEMENTS

This work was supported by The Czech Science Foundation (GACR, projects no. 16-12828S and 17-17139S). VK acknowledges support by the project SVV-2017-260449 (Specific Academic Research Projects).

REFERENCES

[1] TOROPOVA, L. S., ESKIN, D. G., KHARAKTEROVA, M. L. and DOBATKINA, T. V. *Advanced Aluminum Alloys Containing Scandium - Structure and Properties*. Amsterdam: Gordon and Breach Science Publisher, 1998. ISBN 90-5699-089-6.

[2] MICHNA, Š., LUKÁČ, I., OČENÁŠEK, V., KOŘENÝ, R., DRÁPALA, J., SCHNEIDER, H., MIŠKUFOVÁ, A. et al. *Aluminium Materials and Technologies from A to Z*. Prešov: Adin s.r.o., 2007. ISBN 978-80-89244-18-8.

[3] MIAKE, Y., SATO, Y., RYO, T. and KANEKO, K. Effect of heat treatments on the microstructure and formability of Al-Mg-Mn-Sc-Zr alloy. *Micron*. 2017. vol. 101, pp. 151-155. DOI: 10.1016/j.micron.2017.07.003.

[4] LI, Z., ZHANG, Z. and CHEN, X. Improvement in the mechanical properties and creep resistance of Al-Mn-Mg 3004 alloy with Sc and Zr addition. *Materials Science and Engineering A*. 2018. vol. 729, pp. 196-207. DOI: 10.1016/j.msea.2018.07.053.

[5] VAN HUIS, M.A., CHEN, J.H., SLUITER, M.H.F. and ZANDBERGEN, H.W. Phase stability and structural features of matrix-embedded hardening precipitates in Al-Mg-Si alloys in the early stages of evolution. *Acta Materialia*. 2007. vol. 55, pp. 2183-2199. DOI:10.1016/j.actamat.2006.11.019.

[6] VLACH, M., ČÍŽEK, J., SMOLA, B., MELIKHOVA, O., VLČEK, M. KODETOVÁ, V., KUDRNOVÁ, H. and HRUŠKA, P. Heat treatment and age hardening of Al-Si-Mg-Mn commercial alloy with addition of Sc and Zr. *Materials Characterization*. 2017. vol. 129, pp. 1-8. DOI: 10.1016/j.matchar.2017.04.017.

[7] LIU, M., ČÍŽEK, J., CHANG, C.S.T. and BANHART, J. Early stages of solute clustering in an Al-Mg-Si alloy. *Acta Materialia*. 2015. vol. 91, pp. 355-364. DOI: 10.1016/j.actamat.2015.02.019.

[8] VLACH, M., KODETOVÁ, V., KUDRNOVÁ, H., LEIBNER, M., VLČEK, M., ŠÍMA, V., PROCHÁZKA, I., MÁLEK, J. and OČENÁŠEK, V. Mechanical, thermal and electrical characteristics of conventionally cas and cold-rolled 5754-Sc-Zr aluminium alloy. *Defect Diffusion Forum*. 2018. in press.

[9] STARINK, M.J.: The determination of activation energy from linear heating rate experiments: a comparison of the accuracy of isoconversion methods. *Thermochimica Acta*. 2003. vol. 404, no. 1-2, pp. 163-176. DOI: 10.1016/S0040-6031(03)00144-8.

[10] KWON, E.P., WOO, K.D., KIM, S.H., KANG, D.S., LEE, K.J. and JEON, J.Y. The effect of an addition of Sc and Zr on the precipitation behavior of AA6061 alloy. *Metals and Materials International*. 2010. vol. 16, pp. 701-707. DOI: 10.1007/s12540-010-1002-y.